Electronic Supplementary Material (ESI) for Physical Chemistry Chemical Physics.

Supporting Information for

The double exciton state of conjugated chromophores with strong diradical character: insights from TDDFT calculations.

Sofia Canola[a,b], Juan Casado[c] and Fabrizia Negri[a,b]

[a]Università di Bologna, Dipartimento di Chimica 'G. Ciamician', Via F. Selmi, 2, 40126 Bologna, Italy

[b]INSTM, UdR Bologna, Italy.

[c]Department of Physical Chemistry, University of Málaga, Andalucia-Tech, Campus de Teatinos s/n, 29071 Málaga, Spain

Table S1 Absolute energies of the CS and BS equilibrium structures for the systems investigated. The functional used in the calulations is indicatd in each column, the basis set is 6-31G*

molecule	*CS B3LYP*	*BS B3LYP*	*CS CAM-B3LYP*	*BS CAM-B3LYP*
2TIO	-1716.112835	-1716.114497	-1715.587518	-1715.599069
QDTBDT	-2654.823343	-2654.826237	-2654.205229	-2654.221908
FP	-1460.135601	-1460.141536	-1459.271501	-1459.289888
DFB	-1919.852877	-1919.857490	-1918.738459	-1918.752805
BISPHE	-1382.737494	-1382.743254	-1381.914852	-1381.939840
TPQ	-1447.944339	-1447.952670	-1447.121301	-1447.148836
SHZ	-1535.228557	-1535.240897	-1534.329870	-1534.361897
QANTHENE	-2147.467558	-2147.481580	-2146.230673	-2146.264864

Table S2 Tetraradical character computed at different levels of theory (PUHF and PUDFT) for CS and BS optimized structures of the systems investigated. The basis set is 6-31G*

	y_1 PUHF			
Geometry→	CS CAM-B3LYP	CS-B3LYP	BS UCAM-B3LYP	BS UB3LYP
2TIO	0.10	0.11	0.09	0.11
QDTBDT	0.05	0.05	0.04	0.05
FP	0.15	0.17	0.16	0.17
DFB	0.14	0.19	0.19	0.20
BISPHE	0.06	0.06	0.02	0.02
TPQ	0.14	0.14	0.10	0.12
SHZ	0.22	0.24	0.25	0.26
QANTHENE	0.16	0.16	0.14	0.15
	y_1 PUCAM	*y_1 PUB3LYP*	*y_1 PUCAM*	*y_1 PUB3LYP*
Geometry→	CS CAM-B3LYP	CS-B3LYP	BS UCAM-B3LYP	BS UB3LYP
2TIO	0.00	0.00	0.00	0.00
QDTBDT	0.00	0.00	0.00	0.00
FP	0.00	0.00	0.00	0.00
DFB	0.00	0.00	0.00	0.00
BISPHE	0.00	0.00	0.00	0.00
TPQ	0.00	0.00	0.00	0.00
SHZ	0.01	0.00	0.01	0.00
QANTHENE	0.00	0.00	0.00	0.00

Table S3 Computed number of unpaired electrons N_u at different levels of theory for CS and BS optimized structures of the systems investigated. The basis set is 6-31G*

	N_u(UHF)			
Geometry→	CS CAM-B3LYP	CS B3LYP	BS UCAM-B3LYP	BS UB3LYP
2TIO	3.83	4.12	4.21	4.27
QDTBDT	3.57	3.86	3.86	3.98
FP	5.66	6.02	5.98	6.15
DFB	6.49	7.81	7.68	7.95
BISPHE	5.45	5.66	4.68	4.80
TPQ	5.03	5.38	5.20	5.44
SHZ	6.92	7.19	7.13	7.29
QANTHENE	9.12	9.42	9.17	9.44
	N_u(UCAM)	**N_u(UB3LYP)**	**N_u(UCAM)**	**N_u(UB3LYP)**
Geometry→	CS CAM-B3LYP	CS B3LYP	BS UCAM-B3LYP	BS UB3LYP
2TIO	0.87	0.41	1.73	0.84
QDTBDT	1.15	0.62	1.64	0.91
FP	1.33	0.93	1.93	1.34
DFB	1.34	0.91	1.88	1.31
BISPHE	1.65	1.06	1.81	1.18
TPQ	1.54	1.10	1.96	1.43
SHZ	1.96	1.50	2.23	1.67
QANTHENE	2.08	1.68	2.23	1.82

Table S4 Overlap (*S*) between BS frontier molecular orbitals (H_α, H_β, L_α, L_β) obtained from UB3LYP/6-31G* calculations for the singlet open-shell configuration, along with the diradical character computed at PUHF and PUB3LYP levels. All the data are computed employing the BS UB3LYP/6-31G* optimized geometry.

	y_0 *PUHF*	y_0 *PUB3LYP*	$S(H_\alpha,H_\beta)$	$S(L_\alpha,L_\beta)$	$S(H_\alpha,L_\beta)$ and $S(H_\beta,L_\alpha)$
2TIO	0.67	0.10	0,57	-0,62	0,77
QDTBDT	0.68	0.14	0,52	-0,58	0,81
FP	0.80	0.34	0,26	-0,39	0,88
DFB	0.80	0.30	0,23	-0,42	-0,87
BISPHE	0.85	0.26	-0,41	0,46	0,89
TPQ	0.86	0.42	0,14	-0,34	0,89
SHZ	0.87	0.52	-0,23	0,26	0,96
QANTHENE	0.92	0.71	-0,11	0,14	0,96

Table S5 Excited electronic states from TDB3LYP/6-31G* calculations at geometries optimized with the CAM-B3LYP functional. The reference configuration was a restricted or unrestricted configuration as indicated. The double exciton state is identified only in TDUB3LYP (unrestricet open-shell singlet reference configuration) and SF TDUB3LYP (unrestricet open-shell triplet reference configuration)

Excited state character →	*(H→L)*	*(H→L)*	*(H→L)*	*(H→L)*
Type of calculation →	*TD-B3LYP/6-31G**	*TD-B3LYP/6-31G**	*TD-UB3LYP/6-31G**	*exp*
Geometry →	*CS CAM-B3LYP*	*BS UCAM-B3LYP*	*BS UCAM-B3LYP*	
2TIO	2.09	1.66	1.80	1.88[b]
QDTBDT	1.97	1.71	1.72-1.79	1.85[c]
FP	1.61	1.30	1.53	1.48[d]
DFB	1.22	1.00	1.16	1.25[e]
BISPHE	1.41	1.34	1.47	1.43[f]
TPQ	1.74	1.39	1.49	1.46[g]
SHZ	1.21	1.00	1.49	1.50[h]
QANTHENE	0.96	0.75	1.20	1.35[i]
Excited state character →	*(H,H→L,L)*	*(H,H→L,L)*	*(H,H→L,L)*	
Type of calculation →	*TD-UB3LYP/6-31G**	*SF TD-B3LYP/6-31G**	*exp*	
Geometry →	*BS UCAM-B3LYP*	*BS UCAM-B3LYP*		
2TIO	1.14	1.41	1.68[b]	
QDTBDT	1.15	1.57	1.57[c]	
FP	1.18	1.04	1.13[d]	
DFB	0.93	0.86	0.92[e]	
BISPHE	1.07	1.24	1.54[f]	
TPQ	1.21	1.01	1.13[g]	
SHZ	1.33	0.98	1.19[h]	
QANTHENE	0.94	0.76	1.08[i]	

[a] Geometry optimized at CAM-B3LYP/6-31G* (CS) or UCAM-B3LYP/6-31G* (BS) levels of theory; [b]In n-hexane from ref. [1]; [c]Measured in $CHCl_3$ from ref. [2]; [d]In CH_2Cl_2, from ref. [3]; [e]In CH_2Cl_2 from ref. [4]; [f]In $CHCl_3$, from ref [5] [g]Measured in CH_2Cl_2 from ref. [6]; [h]In CH_2Cl_2 from ref. [7]; [i]In CH_2Cl_2 from ref. [8].

Table S6 Computed TD-UB3LYP excitation energies, S^2, wf composition, oscillator strength of the strongly one-photon active excited state (single exciton state or *(H→L))* and the available experimental data for the systems investigated.

Excited state character →		*(H→L)*[a]				
	y_0 PUB3LYP	*E(eV)*	*S^2*	*wf*	*f*	*Exp/eV*
2TIO	0.10	1.81	0.70	0.57Hα →Lα; -0.57Hβ →Lβ	0.883	1.88[b]
QDTBDT	0.14	1.81	0.40	0.55Hα →Lα; -0.55Hβ →Lβ	0.567	1.85[c]
FP	0.34	1.51	0.35	0.67Hα →Lα; -0.67Hβ →Lβ	0.617	1.48[d]
DFB	0.30	1.13	0.79	0.58Hα →Lα; -0.58Hβ →Lβ	0.177	1.25[e]
BISPHE	0.26	1.47	0.04	0.70Hα →Lα; -0.70Hβ →Lβ	0.552	1.43[f]
TPQ	0.42	1.48	0.39	0.68Hα →Lα; -0.68Hβ →Lβ	1.234	1.46[g]
SHZ	0.52	1.49	0.44	0.62Hα →Lα; -0.62Hβ →Lβ	0.086	1.50[h]
QANTHENE	0.71	1.28	0.18	0.71Hα →Lα; -0.71Hβ →Lβ	0.124	1.35[i]

[a] Geometry optimized at UB3LYP/6-31G* (BS) levels of theory; [b]In n-hexane from ref. [1]; [c]Measured in $CHCl_3$ from ref. [2]; [d]In CH_2Cl_2, from ref. [3]; [e]In CH_2Cl_2 from ref. [4]; [f]In $CHCl_3$, from ref [5] [g]Measured in CH_2Cl_2 from ref. [6]; [h]In CH_2Cl_2 from ref. [7]; [i]In CH_2Cl_2 from ref. [8].

Table S7 Computed TD-UB3LYP excitation energies, S^2, wf composition, oscillator strength of the one-photon forbidden excited state (double exciton state or *(H,H→L,L))* for the systems investigated.

Excited state character →		*(H,H→L,L)*[a]				
	y_0 PUB3LYP	*E(eV)*	*S^2*	*wf*	*f*	*Exp/eV*
2TIO	0.10	0.98	0.68	0.70Hα →Lα; 0.70Hβ →Lβ	0.000	1.68[b]
QDTBDT	0.14	1.07	0.48	0.70Hα →Lα; 0.70Hβ →Lβ	0.000	1.57[c]
FP	0.34	1.13	0.38	0.69Hα →Lα; 0.69Hβ →Lβ	0.000	1.13[d]
DFB	0.30	0.91	0.42	0.70Hα →Lα; 0.70Hβ →Lβ	0.001	0.92[e]
BISPHE	0.26	1.03	0.38	0.70Hα →Lα; 0.70Hβ →Lβ	0.000	1.54[f]
TPQ	0.42	1.16	0.35	0.69Hα →Lα; 0.69Hβ →Lβ	0.000	1.13[g]
SHZ	0.52	1.32	0.35	0.62Hα →Lα; 0.62Hβ →Lβ	0.000	1.19[h]
QANTHENE	0.71	1.17	0.30	0.69Hα →Lα; 0.69Hβ →Lβ	0.000	1.08[i]

[a] Geometry optimized at CAM-B3LYP/6-31G* (CS) or UCAM-B3LYP/6-31G* (BS) levels of theory; [b]In n-hexane from ref. [1]; [c]Measured in $CHCl_3$ from ref. [2]; [d]In CH_2Cl_2, from ref. [3]; [e]In CH_2Cl_2 from ref. [4]; [f]In $CHCl_3$, from ref [5] [g]Measured in CH_2Cl_2 from ref. [6]; [h]In CH_2Cl_2 from ref. [7]; [i]In CH_2Cl_2 from ref. [8].

B3LYP

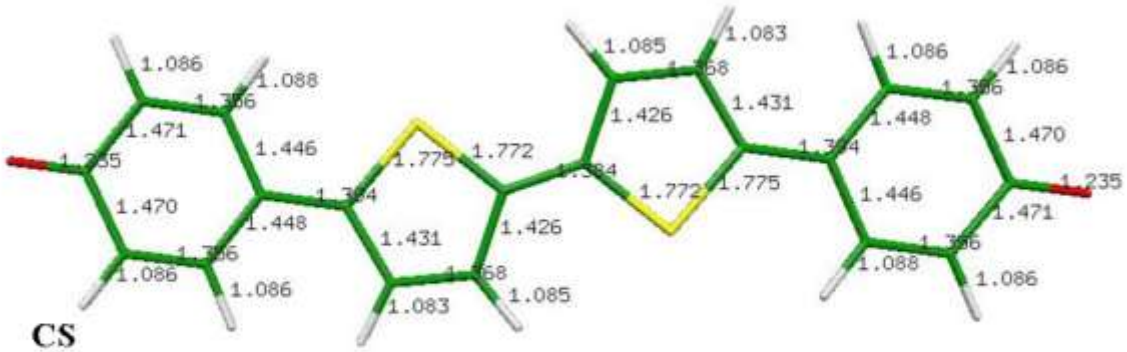

CS

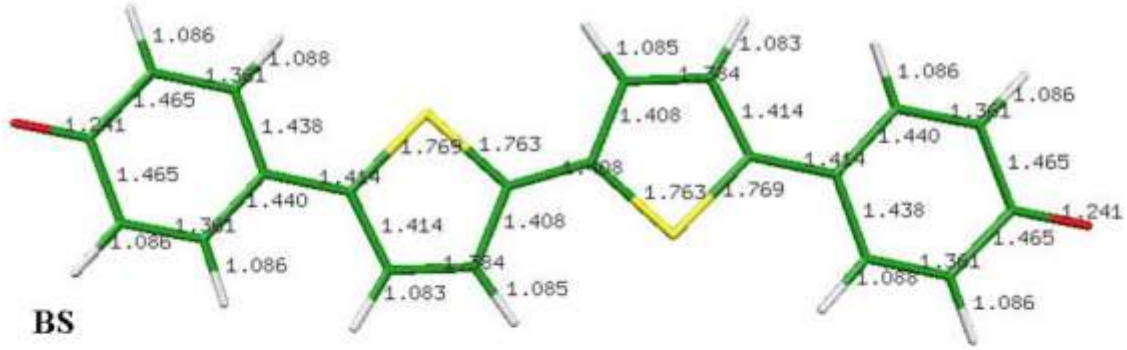

BS

CAM-B3LYP

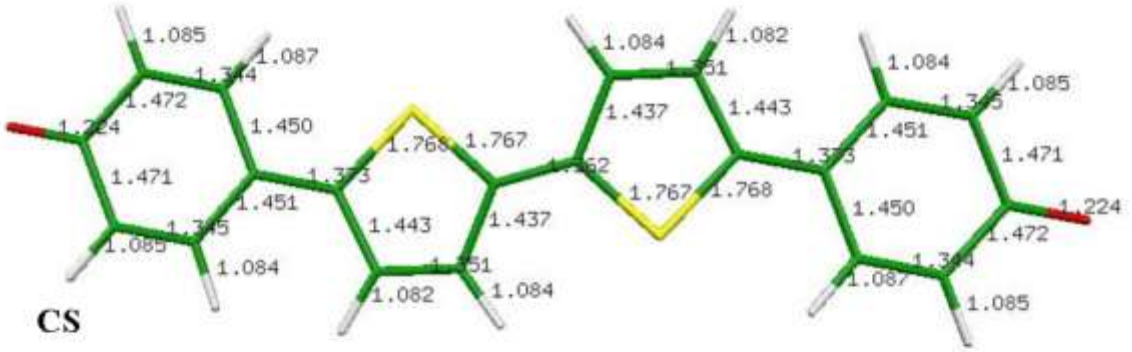

CS

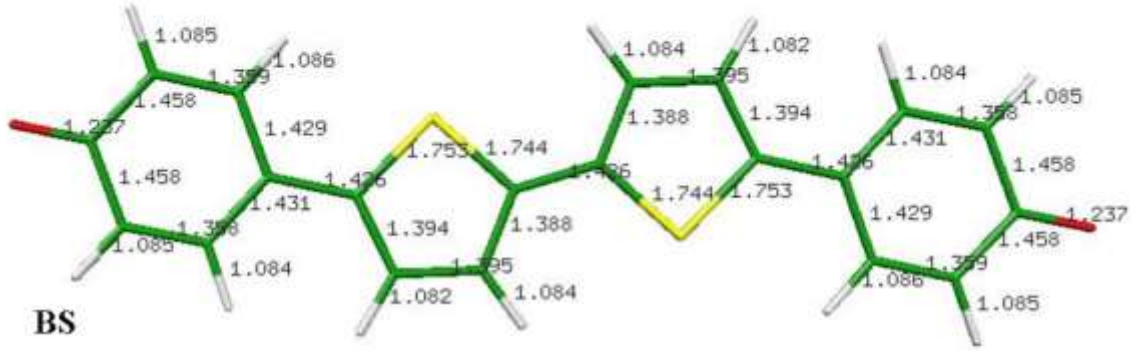

BS

Figure S1. 2TIO: (top) CS and BS equilibrium structures from B3LYP/6-31G* calculations, (bottom) CS and BS equilibrium structures from CAM-B3LYP/6-31G* calculations

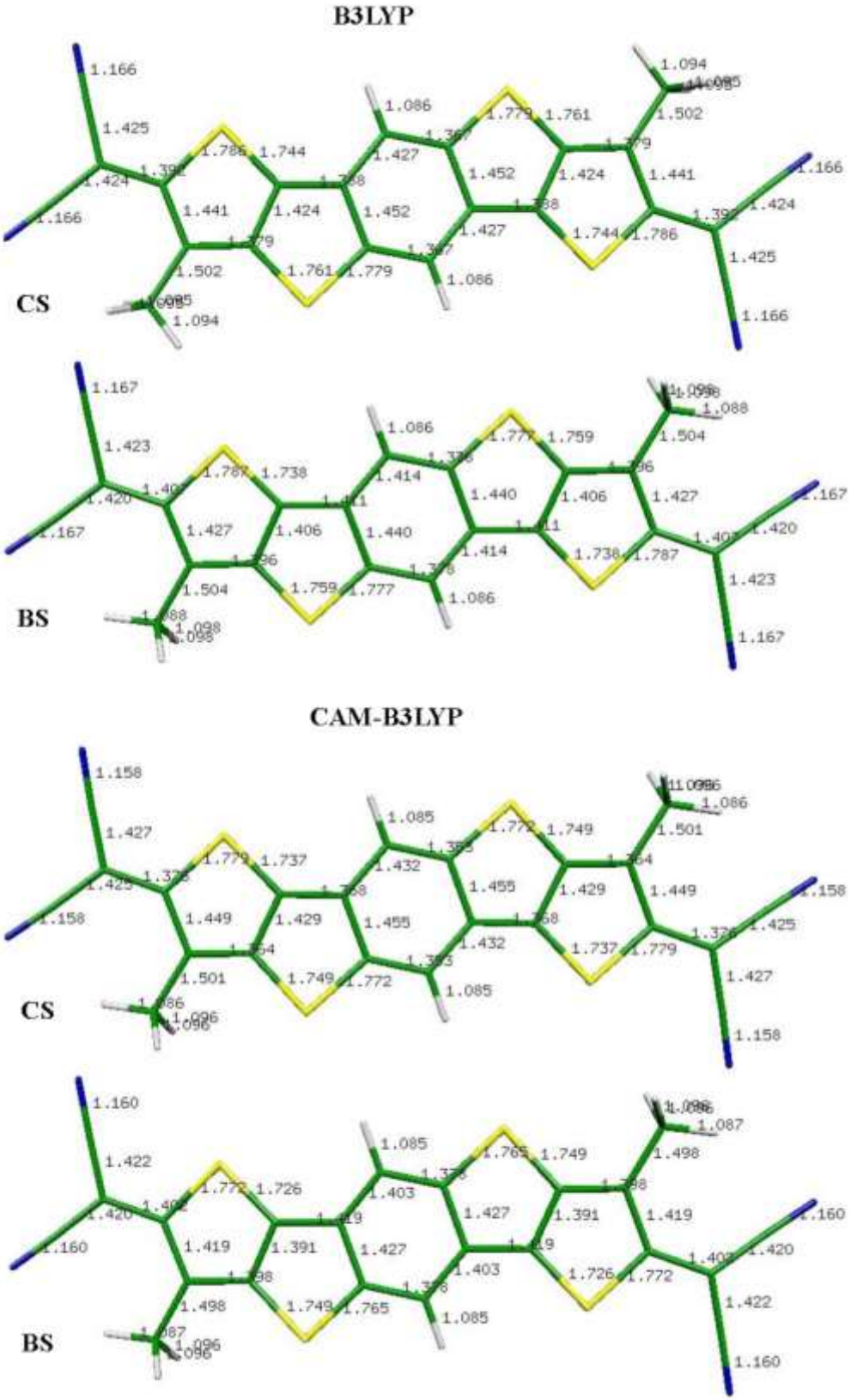

Figure S2. QDTBT: (top) CS and BS equilibrium structures from B3LYP/6-31G* calculations, (bottom) CS and BS equilibrium structures from CAM-B3LYP/6-31G* calculations

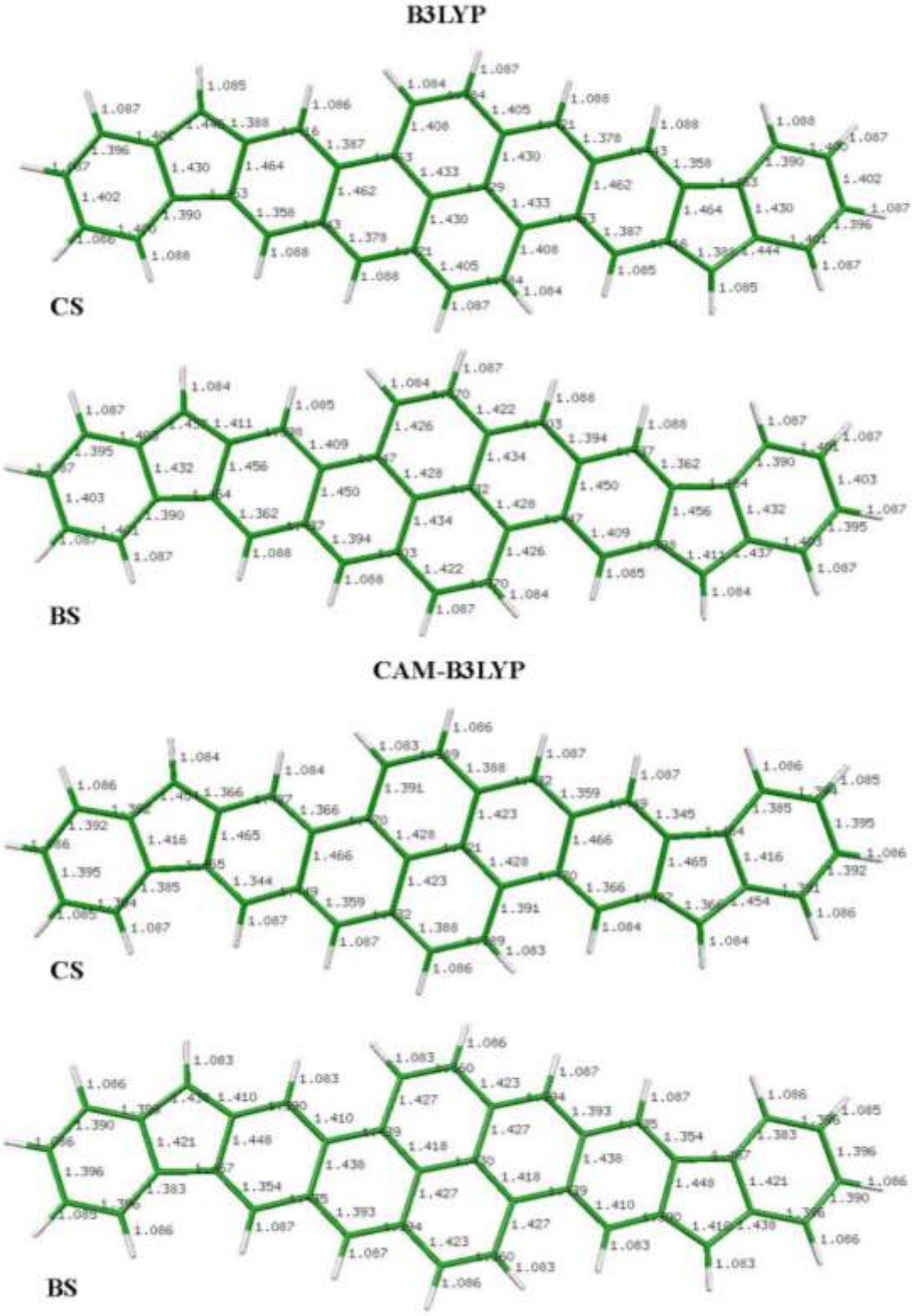

Figure S3. FP: (top) CS and BS equilibrium structures from B3LYP/6-31G* calculations, (bottom) CS and BS equilibrium structures from CAM-B3LYP/6-31G* calculations

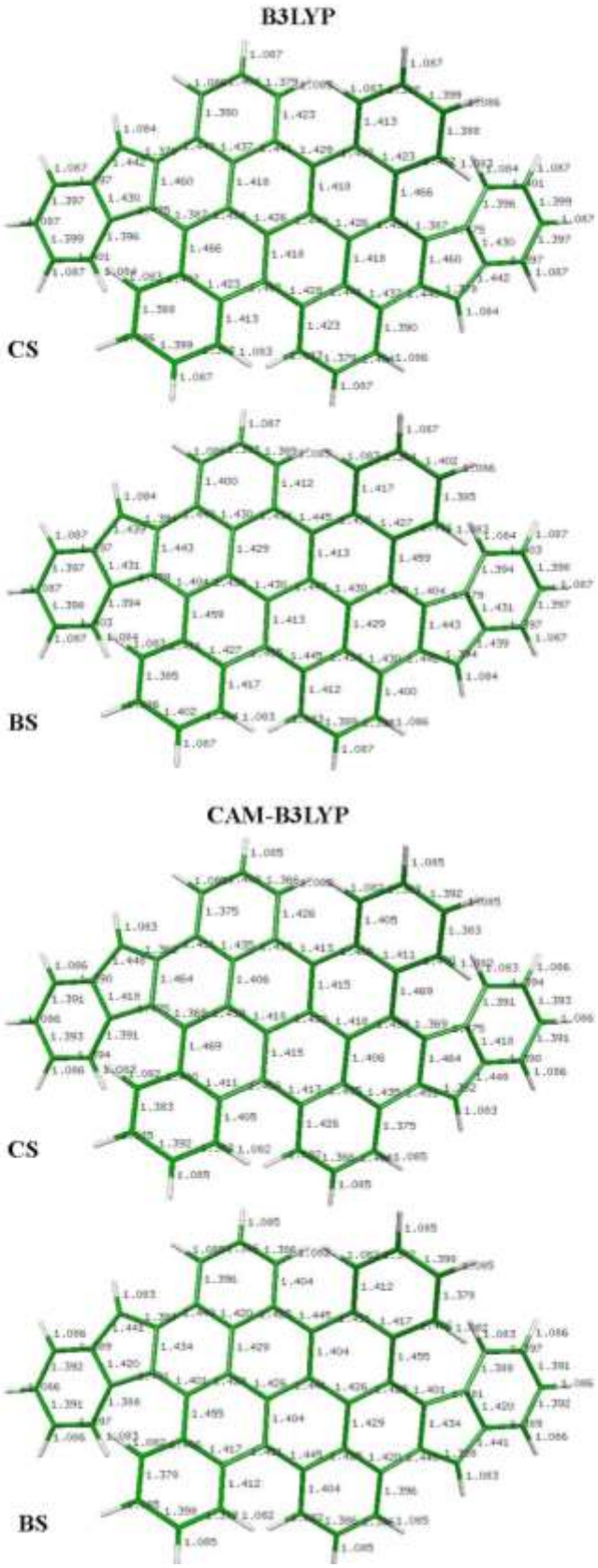

Figure S4. DFB: (top) CS and BS equilibrium structures from B3LYP/6-31G* calculations, (bottom) CS and BS equilibrium structures from CAM-B3LYP/6-31G* calculations

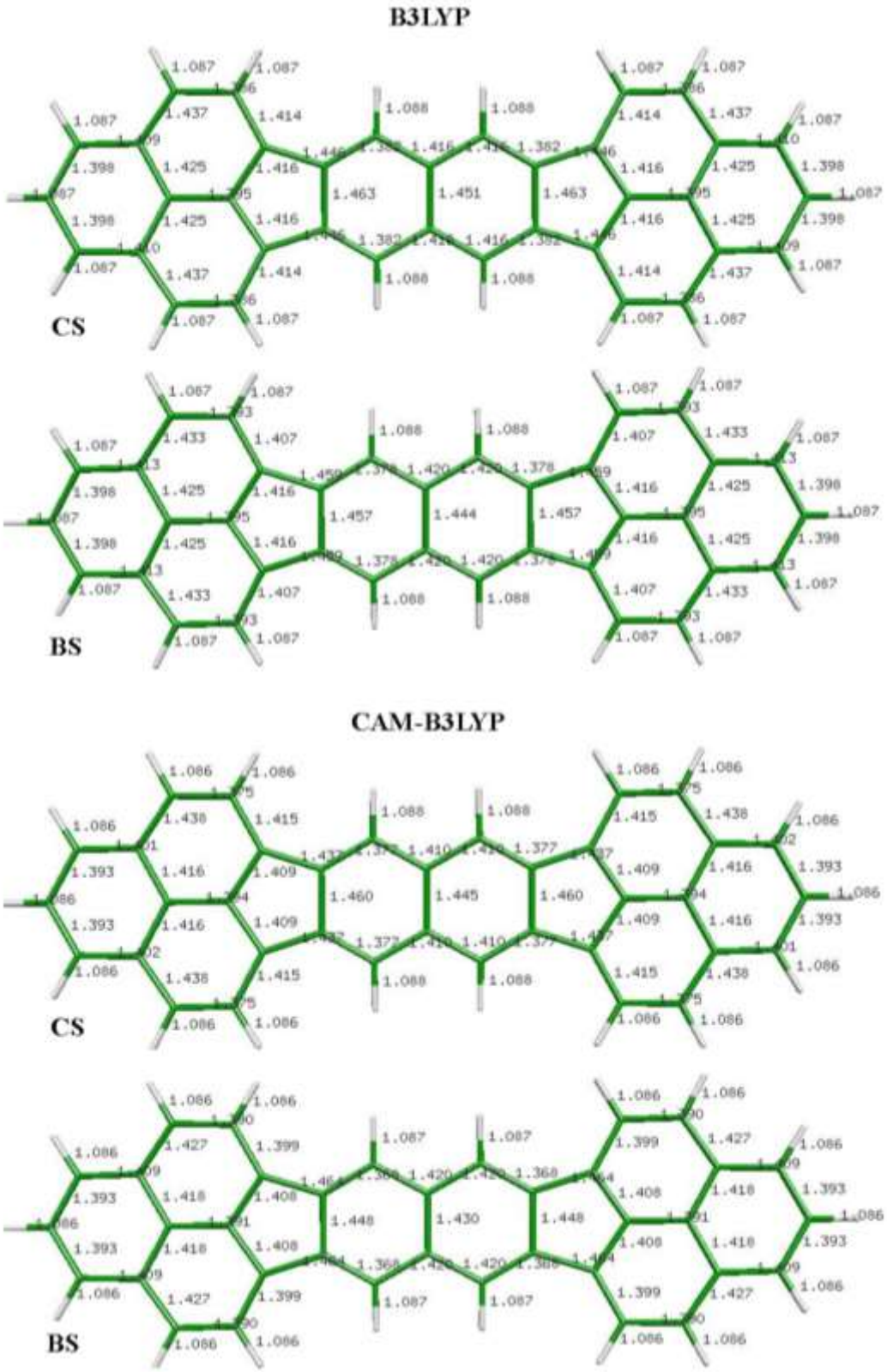

Figure S5. BISPHE: (top) CS and BS equilibrium structures from B3LYP/6-31G* calculations, (bottom) CS and BS equilibrium structures from CAM-B3LYP/6-31G* calculations

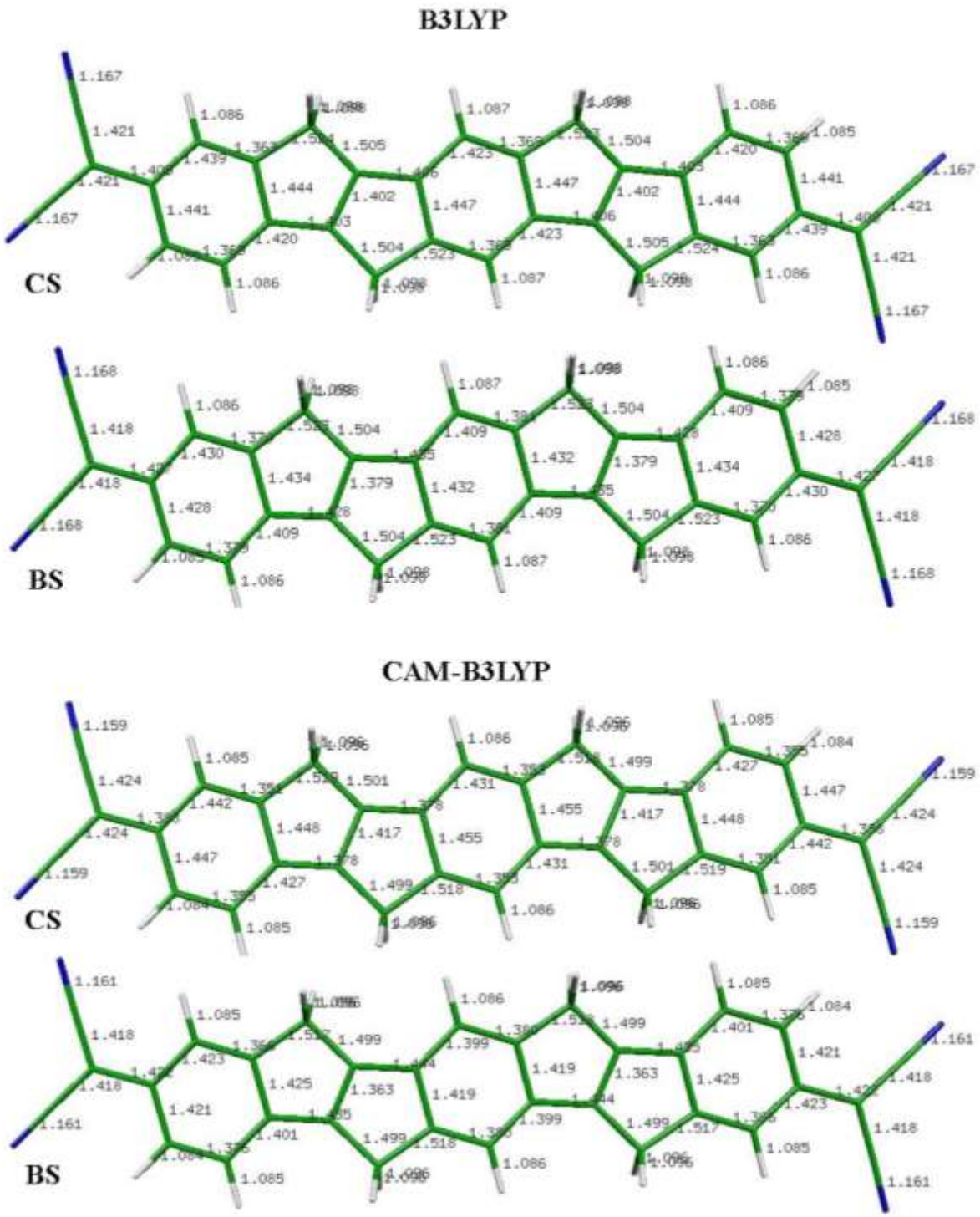

Figure S6. TPQ (top) CS and BS equilibrium structures from B3LYP/6-31G* calculations, (bottom) CS and BS equilibrium structures from CAM-B3LYP/6-31G* calculations

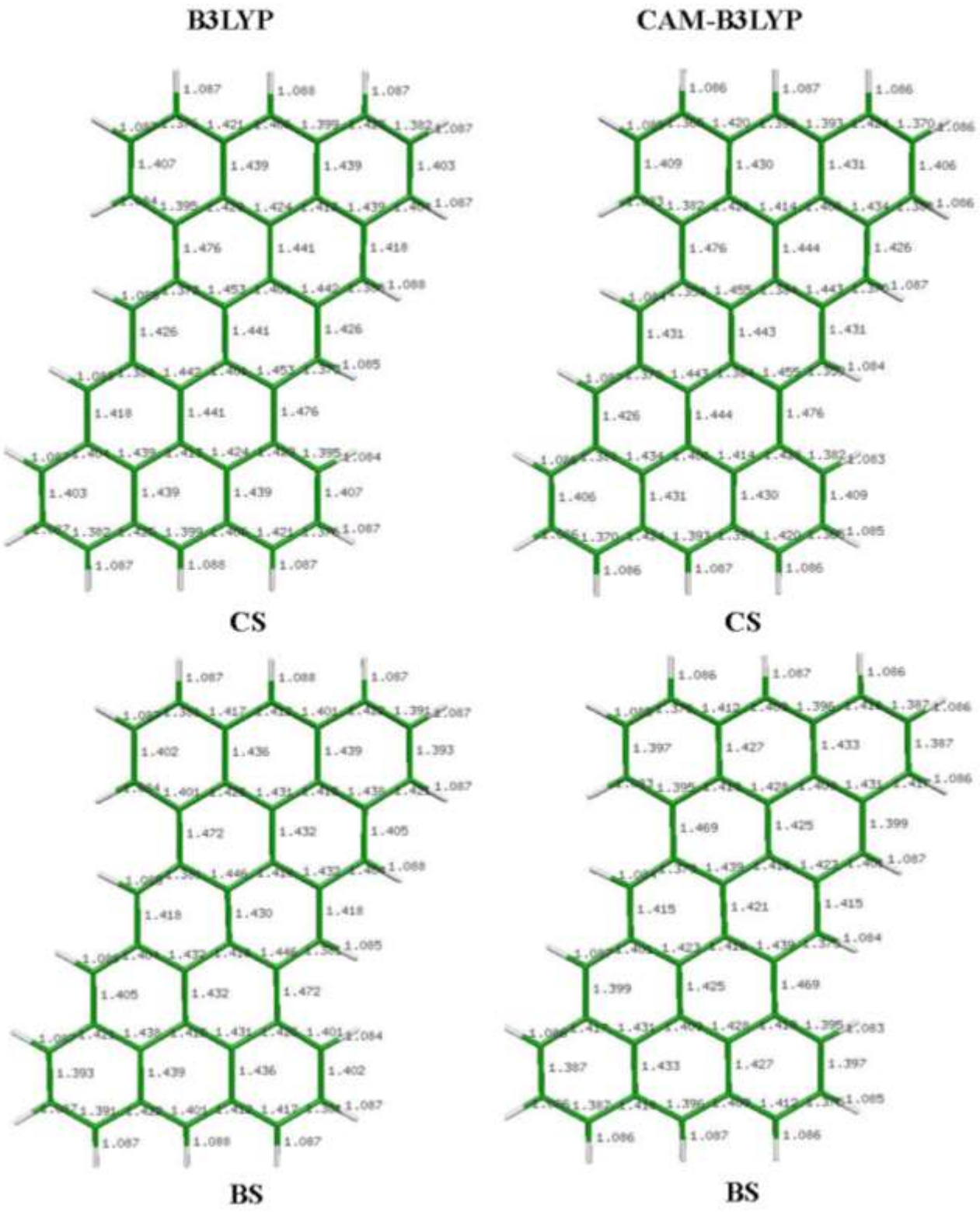

Figure S7. SHZ: (left) CS and BS equilibrium structures from B3LYP/6-31G* calculations, (right) CS and BS equilibrium structures from CAM-B3LYP/6-31G* calculations

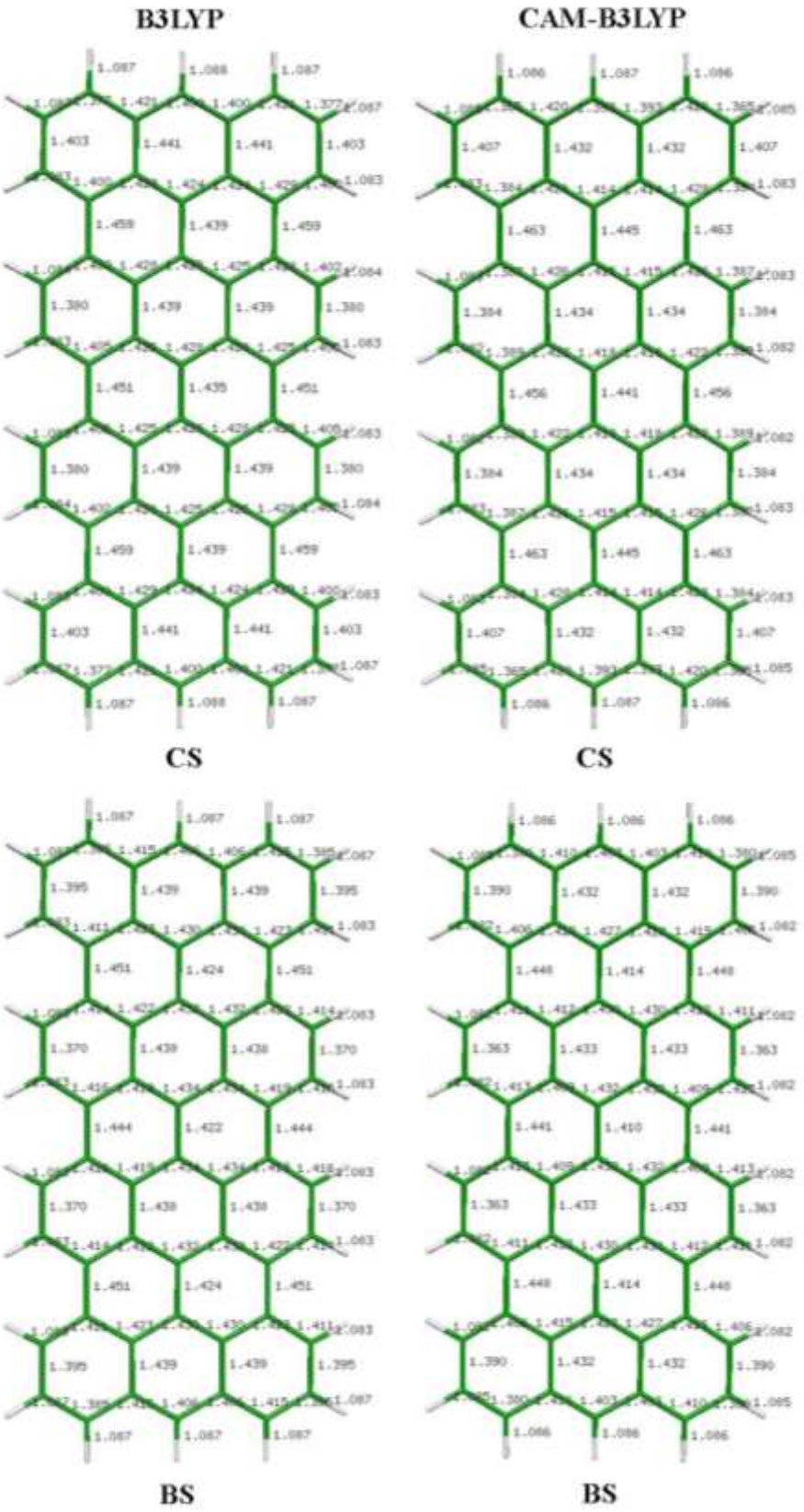

Figure S8. QANTHENE: (left) CS and BS equilibrium structures from B3LYP/6-31G* calculations, (right) CS and BS equilibrium structures from CAM-B3LYP/6-31G* calculations

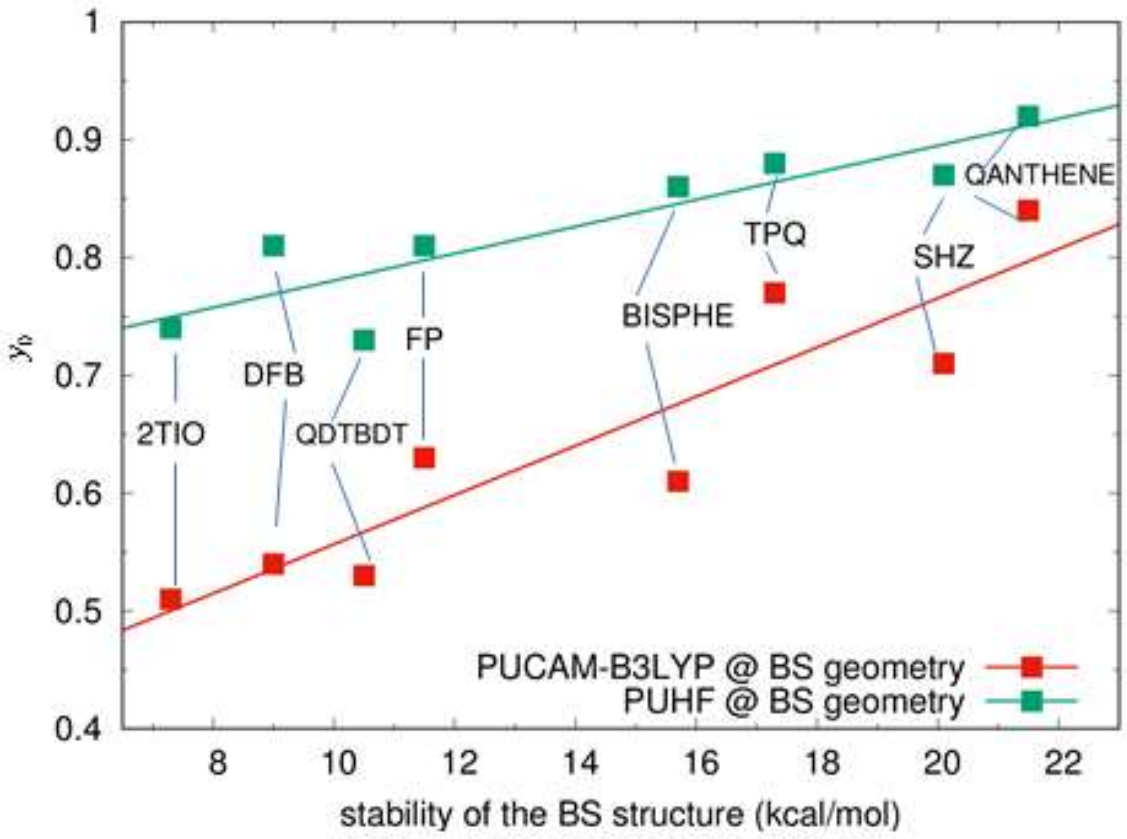

Figure S9. Correlation between the y_0 value computed at PUHF (green squares) or PUCAM-B3LYP (red squares) level and the computed stabilization of the BS structure with respect to the CS structure, both optimized at CAM-B3LYP/6-31G* level.

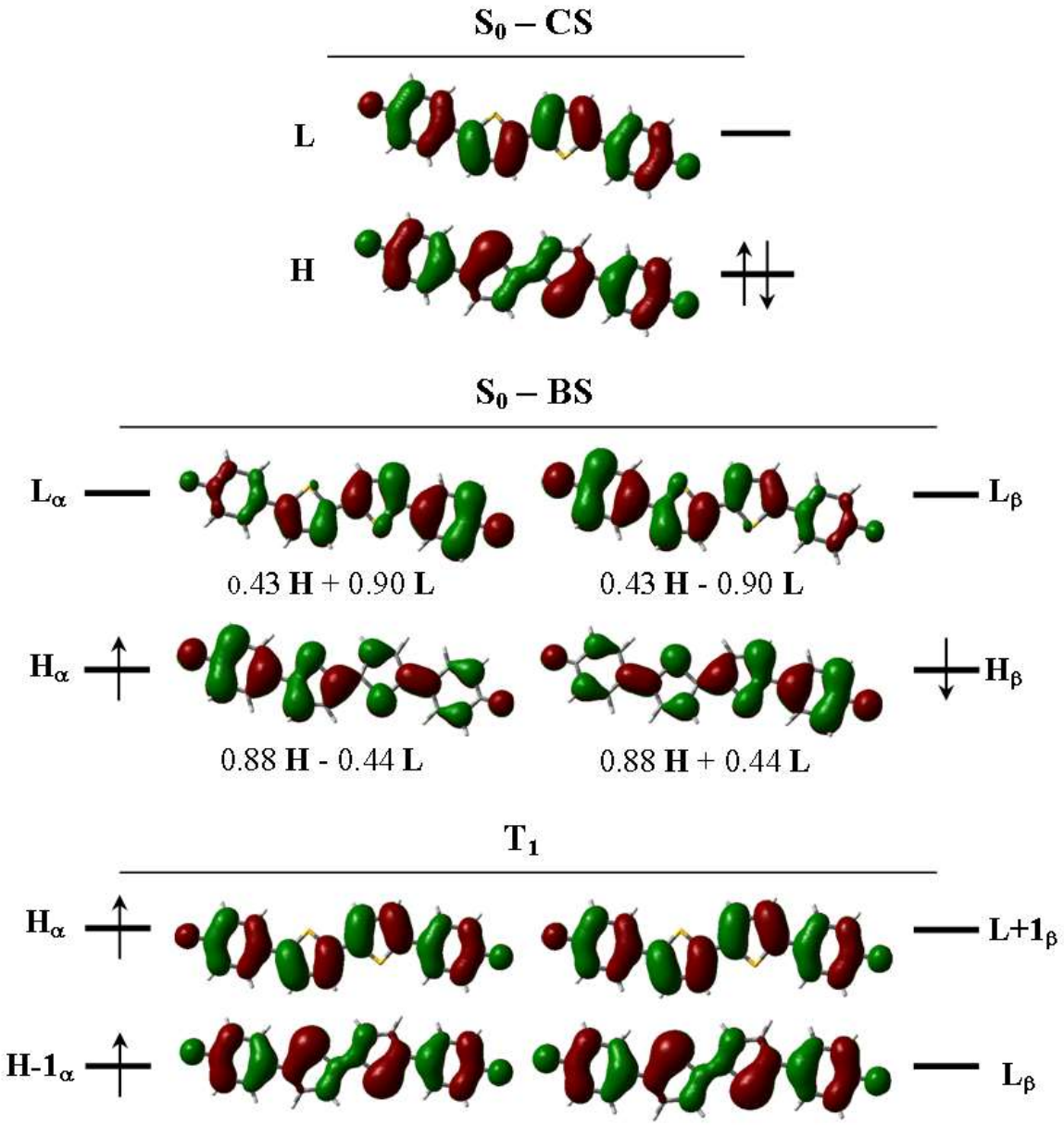

Figure S10. Frontier molecular orbitals of 2TIO computed with (top) a CS singlet reference configuration, (middle) a BS singlet open-shell configuration and (bottom) a triplet configuration, at the optimized BS UB3LYP geometry of the singlet ground state ($y_0(PUHF) = 0.67$). Each localized orbital (BS) is also expressed as a linear combination of the delocalized (CS) orbitals.

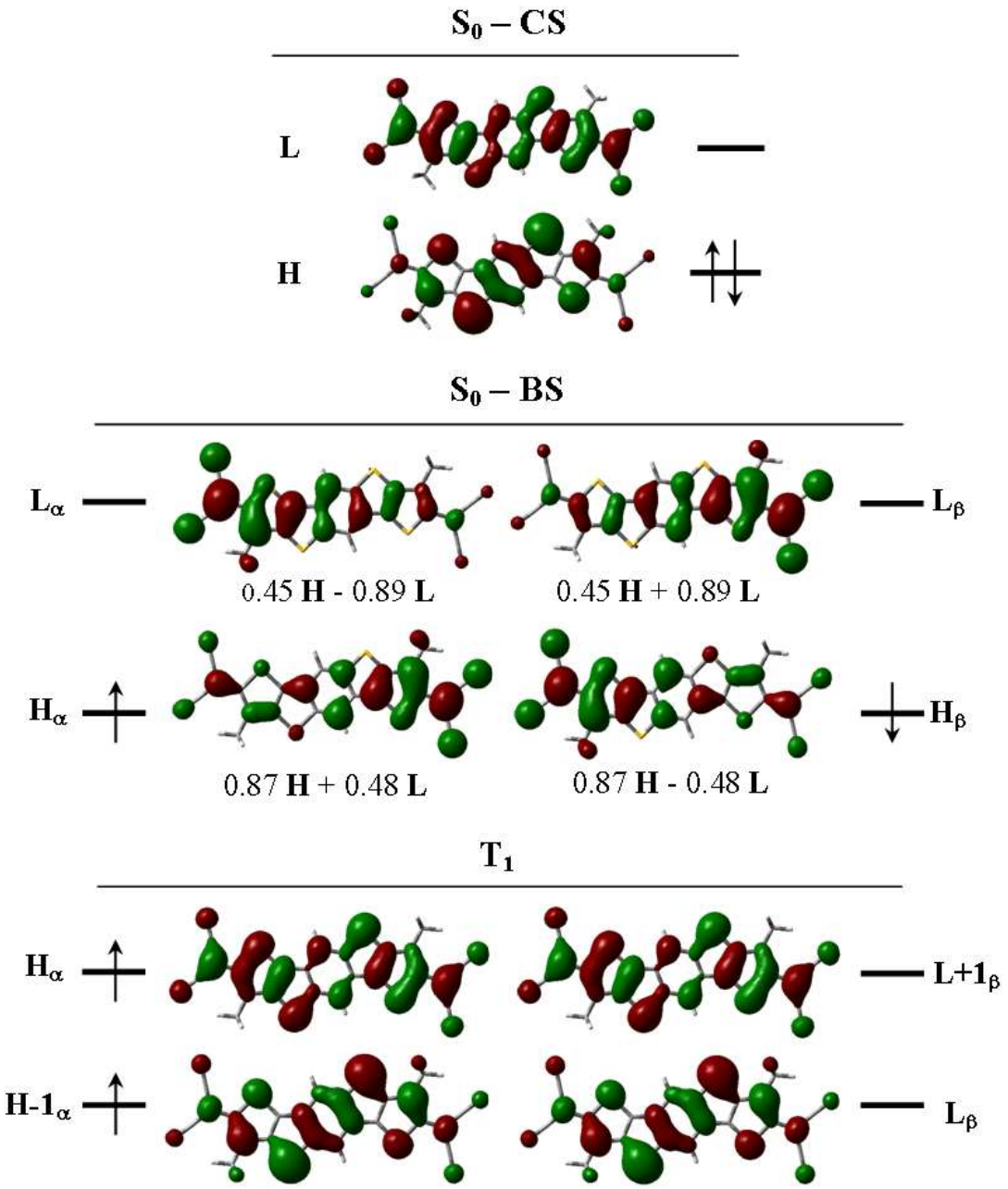

Figure S11. Frontier molecular orbitals of QDTBDT computed with (top) a CS singlet reference configuration, (middle) a BS singlet open-shell configuration and (bottom) a triplet configuration, at the optimized BS UB3LYP geometry of the singlet ground state ($y_0(PUHF) = 0.71$). Each localized orbital (BS) is also expressed as a linear combination of the delocalized (CS) orbitals.

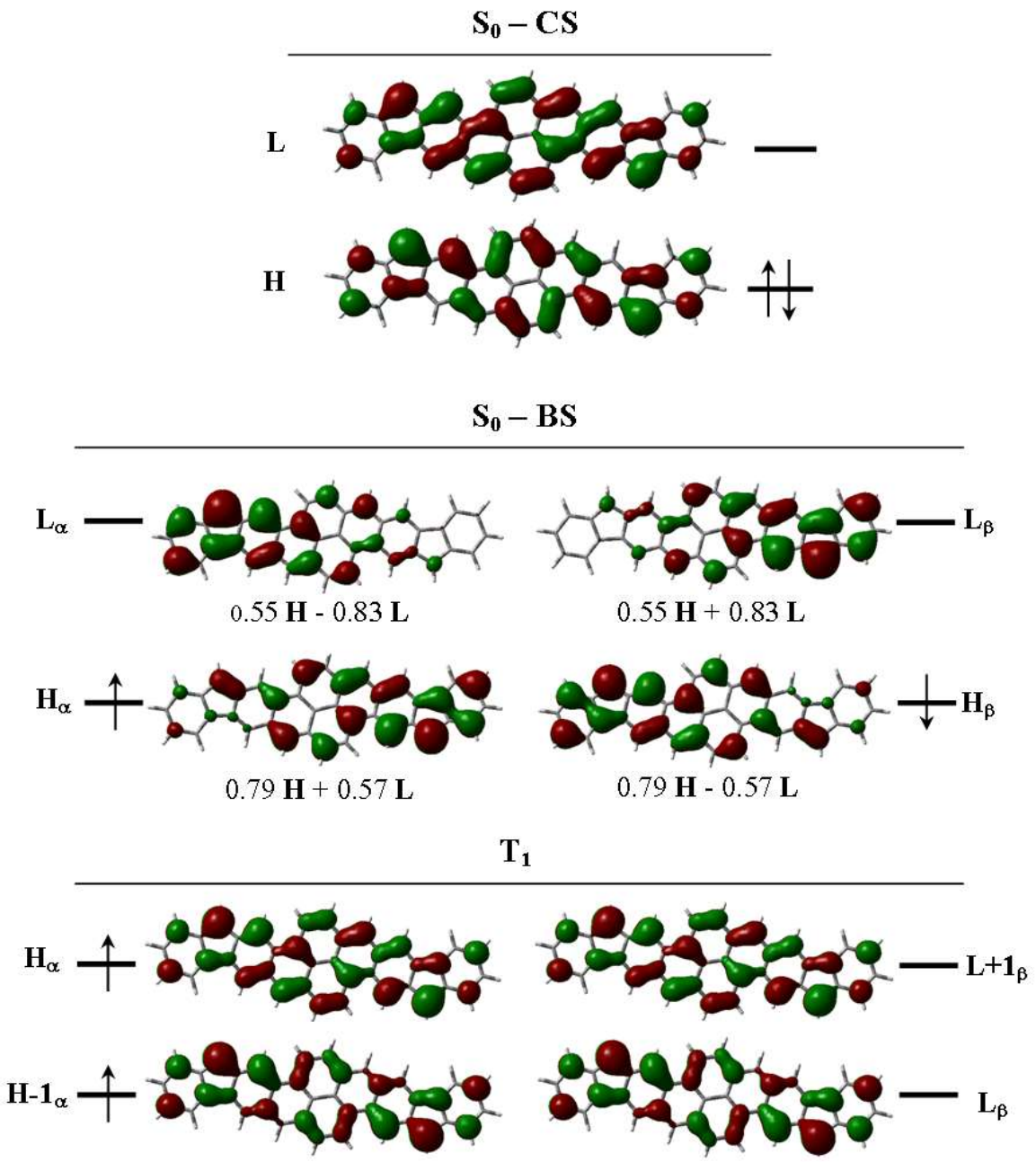

Figure S12. Frontier molecular orbitals of FP computed with (top) a CS singlet reference configuration, (middle) a BS singlet open-shell configuration and (bottom) a triplet configuration, at the optimized BS UB3LYP geometry of the singlet ground state ($y_0(PUHF) = 0.80$). Each localized orbital (BS) is also expressed as a linear combination of the delocalized (CS) orbitals.

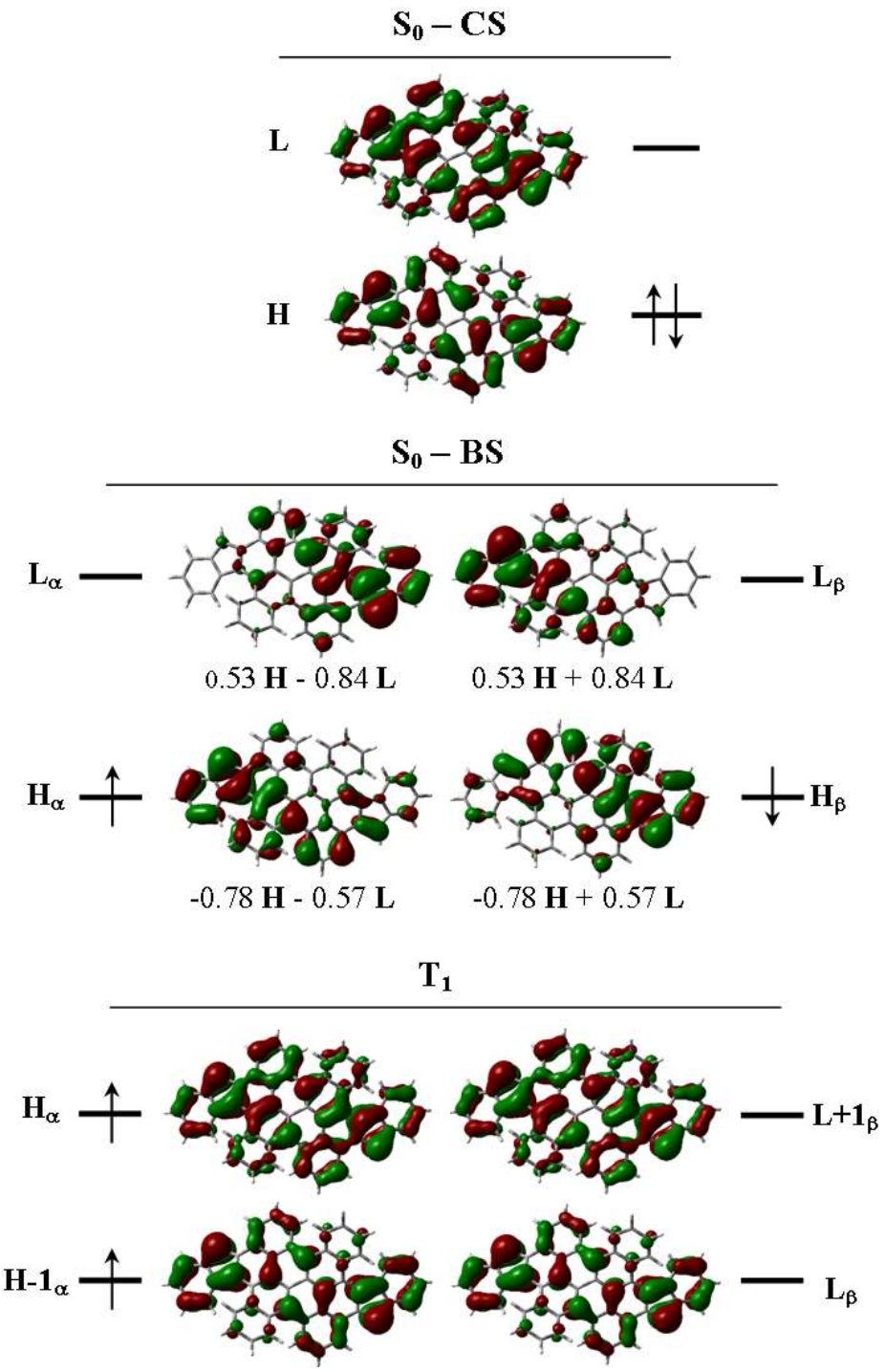

Figure S13. Frontier molecular orbitals of DFB computed with (top) a CS singlet reference configuration, (middle) a BS singlet open-shell configuration and (bottom) a triplet configuration, at the optimized BS UB3LYP geometry of the singlet ground state ($y_0(PUHF) = 0.80$). Each localized orbital (BS) is also expressed as a linear combination of the delocalized (CS) orbitals.

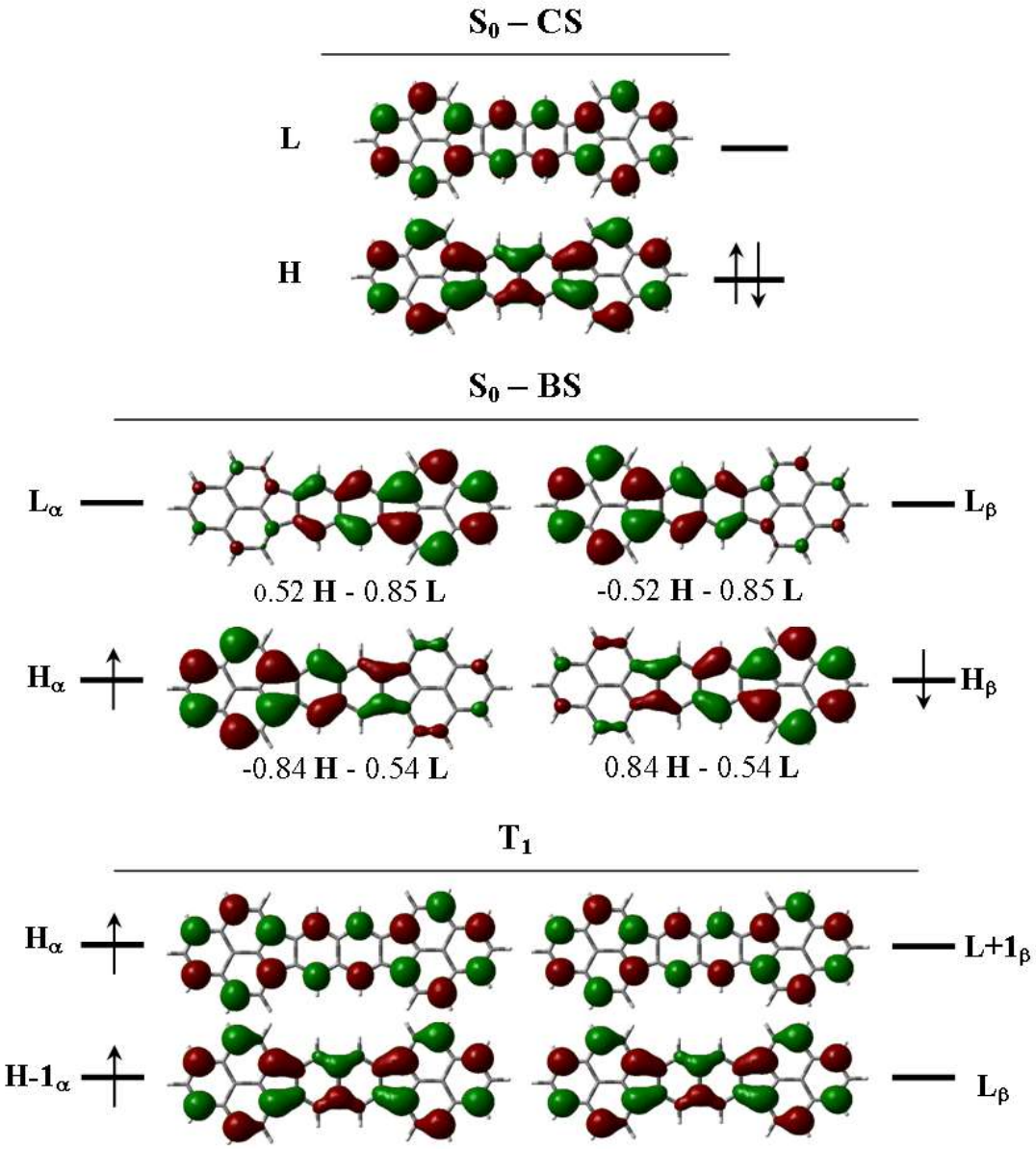

Figure S14. Frontier molecular orbitals of BISPHE computed with (top) a CS singlet reference configuration, (middle) a BS singlet open-shell configuration and (bottom) a triplet configuration, at the optimized BS UB3LYP geometry of the singlet ground state ($y_0(PUHF) = 0.85$). Each localized orbital (BS) is also expressed as a linear combination of the delocalized (CS) orbitals.

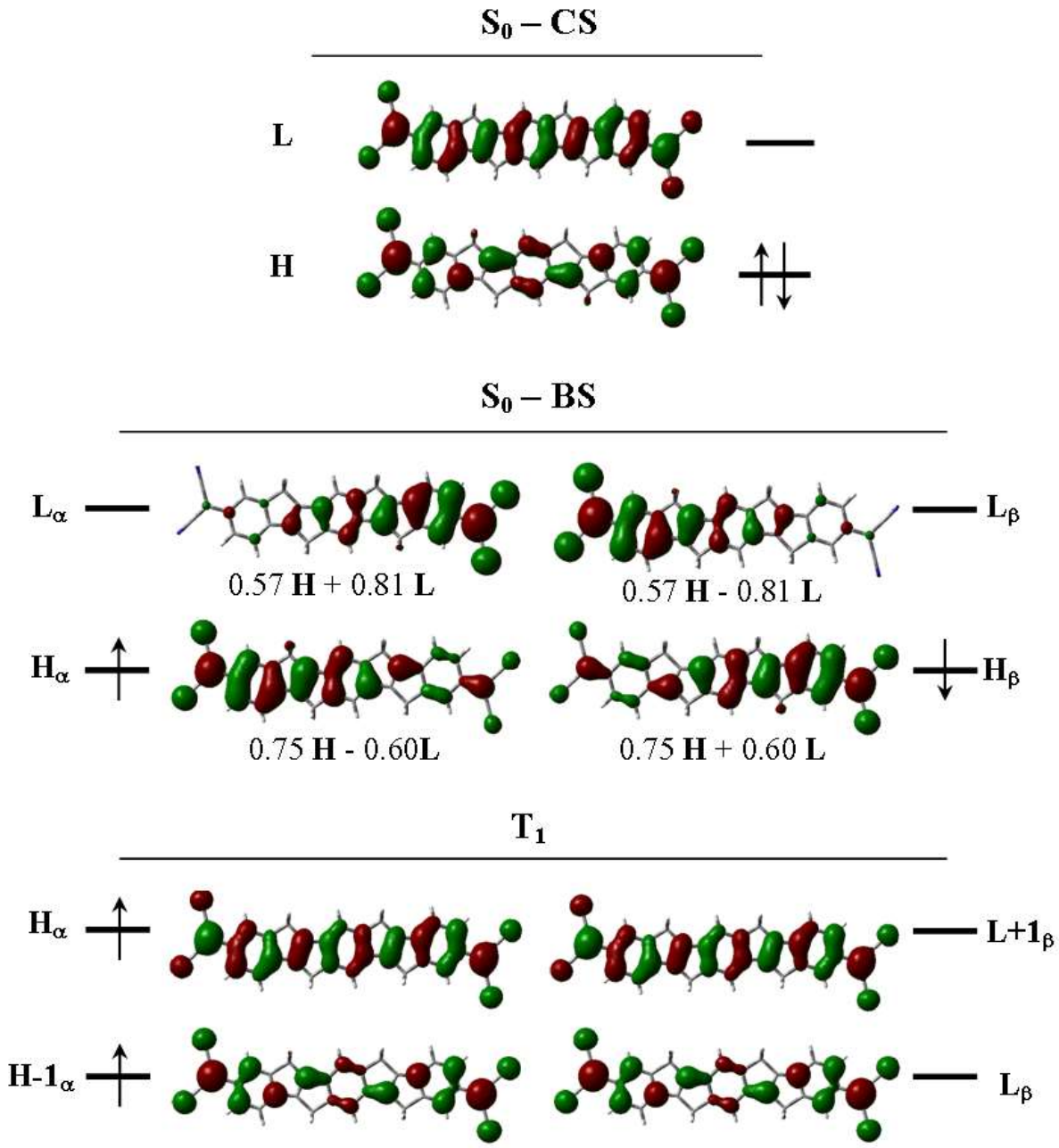

Figure S15. Frontier molecular orbitals of TPQ computed with (top) a CS singlet reference configuration, (middle) a BS singlet open-shell configuration and (bottom) a triplet configuration, at the optimized BS UB3LYP geometry of the singlet ground state ($y_0(PUHF) = 0.86$). Each localized orbital (BS) is also expressed as a linear combination of the delocalized (CS) orbitals.

References

1 S. Di Motta, F. Negri, D. Fazzi, C. Castiglioni and E. V. Canesi, "Biradicaloid and Polyenic Character of Quinoidal Oligothiophenes Revealed by the Presence of a Low-Lying Double-Exciton State", *J. Phys. Chem. Lett*. 2010, **1**, 3334-3339.

2 J. Li, X. Qiao, Y. Xiong, H. Li and D. Zhu, "Five-Ring Fused Tetracyanothienoquinoids as High-Performance and Solution-Processable n-Channel Organic Semiconductors: Effect of the Branching Position of Alkyl Chains", *Chem. Mater.*, 2014, **26**, 5782-5788.

3 P. Hu, S. Lee, T. S. Herng, N. Aratani, T. P. Gonçalves, Q. Qi, X. Shi, H. Yamada, K.-W. Huang, J. Ding, D. Kim and J. Wu, "Toward Tetraradicaloid: The Effect of Fusion Mode on Radical Character and Chemical Reactivity", *J. Am. Chem. Soc.*, 2016, **138**, 1065−1077.

4 J. Ma, J. Liu, M. Baumgarten, Y. Fu, Y-Z. Tan, K. S. Schellhammer, F. Ortmann, G. Cuniberti, H. Komber, R. Berger, K. Müllen and X. Feng, "A Stable Saddle-Shaped Polycyclic Hydrocarbon with an Open-Shell Singlet Ground State", *Angew. Chem. Int. Ed.*, 2017, **129**, 3328-3332.

5 K. Kamada, K. Ohta, A. Shimizu, T. Kubo, R. Kishi, H. Takahashi, E. Botek, B. Champagne and M. Nakano, "Singlet Diradical Character from Experiment", *J. Phys. Chem. Lett.* 2010, **1**, 937-940.

6 X. Zhu, H. Tsuji, K. Nakabayashi, S.-i Ohkoshi and E. Nakamura, "Air- and Heat-Stable Planar Tri-*p*-quinodimethane with Distinct Biradical Characteristics", *J. Am. Chem. Soc.* 2011, **133**, 16342-16345.

7 W. Zeng, Z. Sun, T. S. Herng, T. P. Gonçalves, T. Y. Gopalakrishna, K.-W. Huang, J. Ding and J. Wu, "Super-heptazethrene", *Angew. Chem. Int. Ed.*, 2016, **55**, 8615-8619.

8 A. Konishi, Y. Hirao, K. Matsumoto, H. Kurata, R. Kishi, Y. Shigeta, M. Nakano, K. Tokunaga, K. Kamada and T. Kubo, "Synthesis and Characterization of Quarteranthene: Elucidating the Characteristics of the Edge State of Graphene Nanoribbons at the Molecular Level", *J. Am. Chem. Soc*. 2013, **135**, 1430-1437.